JOURNAL OF VIROLOGY, Nov. 1995, p. 7132–7137 Vol. 69, No. 11
0022-538X/95/$04.00+0

Evi-5, a Common Site of Retroviral Integration in AKXD T-Cell Lymphomas, Maps near *Gfi-1* on Mouse Chromosome 5

XIAOBEI LIAO,† ARTHUR M. BUCHBERG,‡ NANCY A. JENKINS, AND NEAL G. COPELAND*

Mammalian Genetics Laboratory, ABL-Basic Research Program, NCI-Frederick Cancer Research and Development Center, Frederick, Maryland 21702

Received 2 June 1995/Accepted 28 July 1995

We have identified a novel common site of retroviral integration, *Evi-5*, in AKXD T-cell lymphomas. All proviruses located at *Evi-5* are clustered within a 7-kb genomic region and, where determined, are oriented in the same transcriptional direction. Interspecific backcross analysis localized *Evi-5* to mouse chromosome 5, where it cosegregated with another common viral integration site, *Gfi-1*. *Gfi-1* encodes a novel zinc finger transcription factor whose expression is thought to be important for interleukin-2 signaling. Physical mapping studies showed that *Evi-5* is located approximately 18 kb upstream of *Gfi-1*, and Southern analysis showed that *Gfi-1*, like *Evi-5*, is a common integration site in AKXD T-cell tumors. With one exception, *Evi-5* and *Gfi-1* integrations were mutually exclusive. Ten of the tumors with *Evi-5* or *Gfi-1* integrations also harbored viral integrations at other common integration sites causally associated with T-cell disease. These results are consistent with the hypothesis that T-cell lymphomagenesis is a multistep disease and that viral integration at *Evi-5* or *Gfi-1* is causally associated with this disease process.

Inbred mouse strains that have high spontaneous incidences of retrovirally induced disease represent valuable model systems for the identification of novel disease genes. The retroviruses that induce these diseases do not carry oncogenes in their genomes; instead, they induce disease via insertional mutagenesis of cellular proto-oncogenes or tumor suppressor genes (reviewed in references 6, 23, 38, and 47). The disease genes that are affected by viral integration in these tumors can thus be identified as common sites of retroviral integration in tumor DNAs.

One strain that is particularly valuable for the study of retrovirally induced myeloid disease is BXH2. BXH2 mice have the highest spontaneous incidence of retrovirally induced myeloid leukemia of any known inbred mouse strain (1). BXH2 is a recombinant inbred strain derived from a cross between C57BL/6J and C3H/HeJ mice (3). Although the leukemia incidence in the two parental strains is low, greater than 95% of BXH2 mice die of a myelomonocytic leukemia by 1 year of age (1, 30). The high incidence of myeloid leukemia in BXH2 mice is causally associated with the expression of a B-ecotropic murine leukemia virus (MuLV) that is horizontally transmitted in this strain from mother to offspring either through in utero infection or through the mother's milk (2, 24).

Another set of inbred mouse strains that have proven valuable for the study of retrovirally induced myeloid tumors, in addition to T- and B-cell leukemias, are the AKXD recombinant inbred strains (15, 37). These strains were derived by crossing mice from two inbred mouse strains that differ significantly in their lymphoma incidences, AKR/J and DBA/2J. AKR/J is the prototypic highly lymphomatous inbred mouse strain; nearly all of these animal develop T-cell lymphomas by 7 to 16 months of age. DBA/2J is a strain with a low incidence of lymphoma.

The high incidence of lymphomas in AKR/J mice is causally associated with the expression of two endogenous ecotropic MuLV loci, *Emv-11* and *Emv-14* (25). Recombinant viruses termed mink cell focus-forming (MCF) viruses have also been identified in both preleukemic and leukemic thymuses of AKR/J mice (18–20). MCF viruses are not encoded directly in the AKR/J germ line but are generated by multiple recombination events involving an ecotropic virus and at least two endogenous nonecotropic proviruses (12–14, 39, 45, 46). Whereas AKR ecotropic viruses are weakly leukemogenic when injected into newborn mice, MCF viruses are highly leukemogenic (21), suggesting that the generation of MCF viruses is an important event in predisposing AKR mice to the development of T-cell lymphomas.

Among 21 highly lymphomatous AKXD strains available for study, 6 strains die predominantly of T-cell disease, like the AKR/J parent. In contrast, seven strains die predominantly of B-cell disease, one dies predominantly of myeloid disease, and seven die of a mixture of T- and B-cell diseases (15, 37). As expected from the results with AKR/J mice, somatic MCF proviruses are often identified in AKXD T-cell lymphomas, while somatic ecotropic proviruses are identified primarily in lymphomas of the other cell types (15, 35).

As part of our long-term efforts to identify novel myeloid disease genes by using BXH2 mice as a model system, we cloned a somatic ecotropic provirus from a BXH2 tumor and determined if it was located at a common viral integration site. Surprisingly, this provirus was not located at a common viral integration site in BXH2 tumors but instead defined a common viral integration site that was rearranged primarily in AKXD T-cell lymphomas. Genetic and physical mapping studies showed that this common site was linked to, but distinct from, another common viral integration site identified in Moloney MuLV-induced rat T-cell lymphomas. The role of these two common sites in T-cell lymphomagenesis is discussed.

MATERIALS AND METHODS

Mice and tumors. The BXH2 and AKXD recombinant inbred strains were derived and maintained by Benjamin A. Taylor (The Jackson Laboratory, Bar Harbor, Maine). The cell types of BXH2 and AKXD tumors were determined by

* Corresponding author. Phone: (301) 846-1260. Fax: (301) 846-6666.

† Present address: Laboratory of Immunopathology, National Institute of Allergy and Infectious Diseases, Bethesda, MD 20892.

‡ Present address: Department of Microbiology and Immunology, Jefferson Medical College, Philadelphia, PA 19107.

a combination of histopathological and molecular analyses described previously (1, 15, 34).

DNA isolation and Southern blot analysis. High-molecular-weight DNAs were prepared from frozen mouse tissues (25, 37). Bacteriophage and plasmid DNAs were prepared by using standard procedures (41). Yeast DNA was prepared by standard procedures (40). Restriction endonuclease digestions, agarose gel electrophoresis, Southern blot transfers, hybridizations, and washes were performed as described previously (15).

Library construction and screening. A subgenomic library was constructed with DNA from BXH2 tumor 82-6 by cleavage of the DNA to completion with *Eco*RI and subsequent enrichment of DNA fragments of 12 to 15 kb by agarose gel electrophoresis. The size-selected DNA fractions were purified by freezing and phenol extraction (7). The fraction containing the desired somatically acquired retrovirus was identified by Southern blot hybridization with the pEco probe (8), which was then inserted into the *Eco*RI site of lambda dash (Stratagene). The phage was packaged by using Gigapack (Stratagene), and 50,000 recombinant phage were screened. The cloned provirus was then subcloned into the *Eco*RI site of pBluescript SK+ (Stratagene), and subsequently a 1.9-kb genomic flanking region 5′ to the viral integration was subcloned into the *Eco*RI-*Pst*I sites of pBluescript SK+ (Stratagene).

To molecularly clone the unrearranged genomic DNA at *Evi-5* and *Gfi-1*, probe S and probe G were used to screen a C57BL/6J genomic library (27), and overlapping lambda clones, g2, g4, and g19, which span ~50 kb of genomic DNA were isolated.

Probes. pEco, an ecotropic virus-specific probe derived from the ecotropic virus envelope (*env*) gene, has been described elsewhere (8). Probe S is a 610-bp *Sau*3A fragment isolated from a subcloned 1.9-kb *Eco*RI-*Pst*I genomic fragment located upstream of the 82-6 somatic provirus, probe H is an 800-bp *Hin*dIII fragment isolated from the lambda genomic clone g4, and probe G is a subcloned rat genomic DNA fragment (GIE) isolated from sequences located upstream of *Gfi-1* and was a gift from H. Leighton Grimes and Philip N. Tsichlis (Fox Chase Cancer Center, Philadelphia, Pa.).

Restriction mapping. Restriction maps were generated by combinations of Southern blot analysis of genomic DNA and partial digestion of end-labeled lambda genomic clones (41).

YAC cloning. Probe S was used to screen mouse YAC libraries provided by the Reference Library-Data Base, Genome Analysis Laboratory, Imperial Cancer Research Fund (ICRF), London, United Kingdom (33), and a positive clone, ICRFy902C05138, was identified from library no. 902 (31). Yeast colony replication and preparation of filters for Southern hybridizations were performed by procedures described elsewhere (31).

Pulsed-field gel electrophoresis. Cells grown from a single colony of YAC clone ICRFy902C05138 were harvested and embedded in 0.5% (wt/vol) agarose blocks. Restriction endonuclease digestions with *Bss*HII, *Egl*I, *Mlu*I, *Nae*I, *Sal*I, and *Sfi*I were performed, and the products were subjected to contour-clamped homogeneous electric field (CHEF) gel electrophoresis (9) with a CHEF Mapper pulsed-field electrophoresis system (Bio-Rad) as described previously (28). DNA was Southern blotted by standard alkaline transfer methods to Hybond N+ membranes (Amersham), and hybridizations were performed as described previously (24).

Interspecific backcross mapping. Interspecific backcross progeny were generated by mating (C57BL/6J × *Mus spretus*)F_1 females and C57BL/6J males as described previously (10). A total of 205 N_2 mice were used to map the *Evi-5* locus (see Results for details). DNA isolation, restriction enzyme digestion, agarose gel electrophoresis, Southern blot transfer, and hybridization were performed essentially as described previously (25). All blots were prepared with Hybond N+ nylon membranes (Amersham). Probe S was used as the hybridization probe (see Results for details). The probe was labeled with [α-^{32}P]dCTP by random priming (Stratagene); washing was done to a final stringency of 1.0× SSCP (1 × SSCP is 87.7 g of NaCl, 44.1 g of sodium citrate, and 0.0375 g of citric acid in 500 ml)–0.1% sodium dodecyl sulfate at 65°C. A 7.0-kb fragment was detected in *Hin*cII-digested C57BL/6J DNA, and a 5.1-kb fragment was detected in *Hin*cII-digested *M. spretus* DNA. The presence or absence of the 5.1-kb *M. spretus*-specific *Hin*cII fragment in backcross mice was monitored.

Descriptions of the probes and restriction fragment length polymorphisms for the loci linked to *Evi-5*, including those for fibroblast growth factor 5 (*Fgf-5*), growth factor independence 1 (*Gfi-1*), and crystallin beta B2 (*Crybb-2*), have been reported previously (4, 5, 22). Recombination distances were calculated as described previously (17) with the computer program SPRETUS MADNESS. Gene order was determined by minimizing the number of recombination events required to explain the allele distribution patterns.

RESULTS

***Evi-5*, a common site of retroviral integration in AKXD T-cell lymphomas.** As part of our long-term efforts to identify novel myeloid disease genes, we cloned a somatically acquired ecotropic provirus from BXH2 tumor 82-6 (Fig. 1A). Subsequently, we isolated a unique-sequence 610-bp *Sau*3A fragment, termed probe S (Fig. 1A), from the cellular DNA sequences located 5′ of the 82-6 provirus and used it to determine whether the 82-6 provirus was located at a common viral integration site in BXH2 tumors. A panel of 160 *Eco*RV-digested BXH2 tumor DNAs was analyzed by Southern hybridization with probe S. Among the 160 DNAs tested, only tumor 82-6 showed a rearranged fragment (Fig. 1B; data not shown). These results suggested that the 82-6 provirus is not located at a common viral integration site in BXH2 tumors.

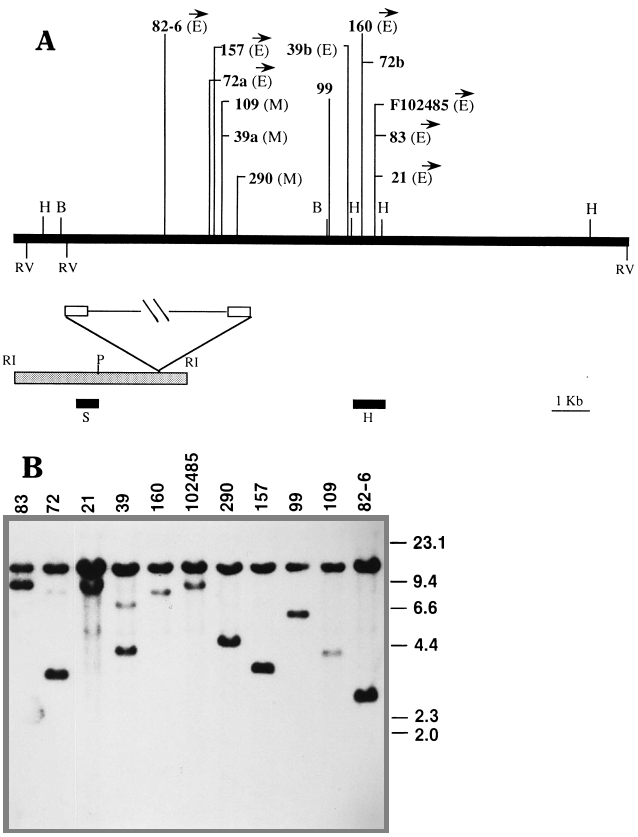

FIG. 1. (A) Restriction map of the *Evi-5* common viral integration site. Abbreviations for restriction endonucleases: B, *Bam*HI; H, *Hin*dIII; RI, *Eco*RI; RV, *Eco*RV; P, *Pst*I. The positions and orientations (5′ to 3′) of proviruses integrated at *Evi-5* are shown above the restriction map. The type of integrated provirus, when known, is also indicated: E, ecotropic provirus; M, MCF provirus. The two proviral integrations in tumors 39 and 72 are arbitrarily labeled a and b. The shaded box below the map represents the provirus-containing *Eco*RI fragment that was cloned from BXH2 tumor 82-6. The provirus is shown by a broken thin line flanked by two open boxes representing viral long terminal repeats. The solid boxes below the map represent the locations of unique-sequence-containing DNA probes derived from the *Evi-5* locus (probes S and H). (B) *Evi-5* rearrangements in BXH2 and AKXD tumors. *Eco*RV-digested tumor DNAs were Southern blotted and hybridized with probe S. The number of each tumor containing a proviral integration at *Evi-5* is listed above the lanes. The unrearranged germ line *Eco*RV fragment is 13 kb. The additional *Eco*RV fragments seen in each tumor indicate virus-induced rearrangements of *Evi-5*. The numbers to the right correspond to the sizes (in kilobases) of *Hin*dIII-digested lambda DNA fragments run in a parallel lane of the same gel.

In addition to the 160 BXH2 tumors, we also screened a panel of 283 AKXD tumors for retrovirally induced rearrangements by using probe S. This panel of AKXD tumors includes about equal numbers of retrovirally induced B- and T-cell lymphomas in addition to a small number of retrovirally induced myeloid tumors (15, 34). Ten of the AKXD tumors screened showed virally induced rearrangements (Fig. 1B; Table 1). Eight of these tumors were T-cell lymphomas, one was a mixed T-cell and myeloid lymphoma, and one was a B-cell lymphoma (Table 1). Thus, while the genomic locus defined by

TABLE 1. Virally induced rearrangements at the *Evi-5* locus in AKXD tumors

Recombinant inbred strain	Tumor no.	Tumor type[a]	Second viral insertion(s)
AKXD3	83	T	*Mlvi-1*
AKXD6	72	T	
AKXD17	21	T	
AKXD17	39	T	*Gfi-1*
AKXD18	160	T	
AKXD21	290	T	*Pvt-1*
AKXD21	102485	T	
AKXD23	157	M/T	*Evi-1*
AKXD27	99	T	*Myc*, *Pim-1*
AKXD27	109	B	
BXH2	82-6	M	

[a] T, T-cell lymphoma; M/T, mixed myeloid and T-cell lymphoma; B, B-cell lymphoma; M, myeloid leukemia.

the 82-6 provirus is not a common viral integration site in BXH2 tumors, it is a common viral integration site in AKXD tumors. This common viral integration site has been designated *Evi-5* (ecotropic viral integration site 5). *Evi-5* rearrangements were detected predominantly in AKXD T-cell lymphomas, suggesting that the *Evi-5* locus harbors a T-cell proto-oncogene or tumor suppressor gene.

Viral integrations at *Evi-5* are clustered within a 7-kb genomic region. The integration site of each provirus located at *Evi-5* was characterized by Southern analysis following digestion with *Eco*RV or *Kpn*I, each of which cut once within the ecotropic viral long terminal repeat, and hybridization with probe S and another probe, probe H, which maps approximately 5 kb downstream of probe S (Fig. 1; see Fig. 4). Tumor DNAs were also digested with *Eco*RI, which does not cut within ecotropic proviruses, in order to confirm that the rearrangements were due to ecotropic viral integration. The results of this analysis are summarized in Fig. 1A. Among the 11 tumors analyzed (Table 1), 9 had single viral insertions, while 2, AKXD tumors 72 and 39, each had two viral insertions (Fig. 1). In the absence of cell lines from these tumors, we are not able to determine whether the two viral insertions occurred in the same cell or in two different subpopulations of the same tumor. All of the proviruses were located within a 7-kb region, and eight appeared to represent ecotropic proviruses. Five of the proviruses generated *Eco*RI restriction fragments that were not consistent with ecotropic virus integration. We presume that these three proviruses are MCF proviruses, which are frequently identified in AKXD T-cell tumors (35).

The orientations of seven of the ecotropic proviruses were determined by Southern analysis following digestion with *Hin*dIII, *Sac*I, or *Bam*HI, each of which cut asymmetrically within the ecotropic provirus. The orientations of the MCF proviruses could not be easily determined because of the variability in the restriction maps of different MCF proviruses. All seven of the ecotropic proviruses analyzed were oriented in the same transcriptional direction.

***Evi-5* maps near *Gfi-1* on mouse chromosome 5.** The mouse chromosomal location of *Evi-5* was determined by interspecific backcross analysis with progeny derived from matings of (C57BL/6J × *M. spretus*)F_1 mice with C57BL/6J mice. This interspecific backcross mapping panel has been typed for over 1,900 loci that are well distributed among all the mouse autosomes and the X chromosome (10, 10a). C57BL/6J and *M. spretus* DNAs were digested with several different restriction enzymes and analyzed by Southern blot hybridization for informative restriction fragment length polymorphisms by using

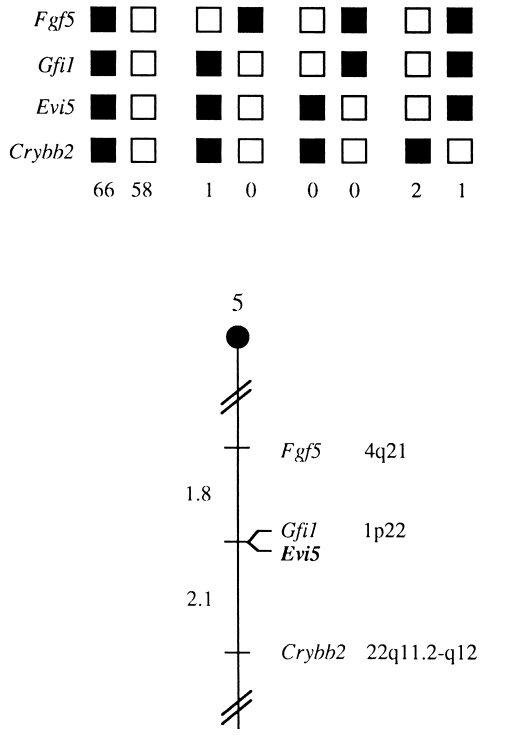

FIG. 2. Mouse chromosomal location of *Evi-5*. (Top) Segregation of *Evi-5* and flanking markers in 128 N_2 (C57BL/6J × *M. spretus*)F_1 × C57BL/6J backcross mice. Each column represents the chromosome identified in the N_2 progeny that was inherited from the (C57BL/6J × *M. spretus*)F_1 female parent. Black boxes represent C57BL/6J alleles; white boxes represent *M. spretus* alleles. Locus symbols are shown on the left. The numbers at the bottom indicate the total number of N_2 mice inheriting each type of chromosome. (Bottom) Partial linkage map of mouse chromosome 5, showing the map location of *Evi-5* and flanking markers (see Results). The map distances (in centimorgans) are indicated on the left of the map, and the map locations of human loci are shown on the right.

probe S. A 5.1-kb *M. spretus*-specific *Hin*cII restriction fragment length polymorphism was used to monitor the segregation of the *Evi-5* locus in backcross mice (see Materials and Methods). The mapping results indicated that *Evi-5* is located on mouse chromosome 5, where it cosegregated with *Gfi-1* in 169 animals typed in common (Fig. 2). Although only 128 mice were typed for every marker shown in the haplotype analysis (Fig. 2, top), up to 193 mice were typed for some pairs of markers. Each locus was analyzed in pairwise combinations for recombination frequencies by using the additional data. The ratios of the total number of mice exhibiting recombinant chromosomes to the total number of mice analyzed for each pair of loci and the most likely gene order are as follows: centromere–*Fgf-5*–3/169–(*Gfi-1* and *Evi-5*)–3/145–*Crybb-2*. The recombination frequencies (expressed as genetic distances in centimorgans ± the standard error) are as follows: *Fgf-5*–1.8 ± 1.0–(*Gfi-1* and *Evi-5*)–2.1 ± 1.2–*Crybb-2*. The fact that no recombinants between *Gfi-1* and *Evi-5* were detected in 169 animals typed in common suggests that the two loci lie within 1.6 centimorgans of each other (95% confidence limit).

Gfi-1, like *Evi-5*, is a common viral integration site that was identified during progression of Moloney MuLV-induced rat interleukin-2 (IL-2)-dependent T-cell lymphoma lines to IL-2-independent growth (16). Proviral integration at *Gfi-1* upregulates the expression of a novel zinc finger protein that is expressed at low levels in IL-2-dependent T-cell lymphoma lines. In mitogen-stimulated splenocytes, *Gfi-1* expression begins to rise 12 h after stimulation and reaches high levels after 50 h.

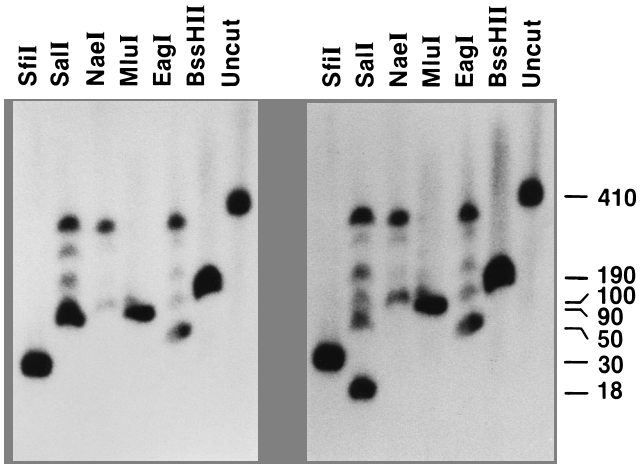

FIG. 3. CHEF analysis of the *Evi-5*–*Gfi-1* region. DNA from YAC clone ICRFy902C05138 was digested with rare-cutter restriction endonucleases, separated by CHEF electrophoresis, and analyzed by Southern blot hybridization. The blot was hybridized with *Evi-5* probe S (left) and then stripped and rehybridized with *Gfi-1* probe G (right). The enzymes used in the analysis are indicated above the lanes. Molecular sizes (in kilobases) are given on the right. Note that both probe S and probe G hybridize to the same 30-kb *Sfi*I fragment.

This result suggests that *Gfi-1* is a downstream target of the IL-2 receptor and may function during the transition from the G_1 to the S phase of the cell cycle. Consistent with this hypothesis, overexpression of *Gfi-1* does not induce expression of IL-2 but does contribute to the emergence of the IL-2-independent phenotype (16).

***Evi-5* and *Gfi-1* represent two different, closely linked common viral integration sites.** In order to determine if *Evi-5* and *Gfi-1* are the same common integration site, one identified in the mouse and one identified in the rat, we generated a restriction enzyme map of the mouse *Gfi-1* locus and compared it with the restriction enzyme map of *Evi-5*. The results of this analysis indicated that the two common integration sites are distinct (data not shown). Next, we isolated a 410-kb YAC clone of mouse genomic DNA by using probe S. The physical distance between the two common integration sites was then determined by CHEF electrophoresis of this 410-kb YAC clone with probe S (Fig. 3, left panel) and a rat *Gfi-1* probe (Fig. 3, right panel). The two pulsed-field gel electrophoresis maps were virtually identical; the only major differences was that the *Evi-5* probe was located on an 80-kb *Sal*I fragment, while the *Gfi-1* probe was located on an 18-kb *Sal*I fragment. The two probes were colocalized to a 30-kb *Sfi*I fragment. These results suggest that the two common sites are located within 30 kb of each other in the genomic DNA.

In order to more precisely determine the physical distance between *Evi-5* and *Gfi-1*, we isolated a number of overlapping genomic lambda clones from the *Evi-5*–*Gfi-1* region (Fig. 4). Three of the clones, g2, g4, and g19, covered 50 kb of genomic DNA. Hybridization of *Evi-5* probes S and H and of *Gfi-1* probe G to this genomic contig allowed us to position *Evi-5* approximately 18 kb upstream of *Gfi-1* (Fig. 4).

***Gfi-1* is a common viral integration site in AKXD lymphomas.** To determine if *Gfi-1* was a common viral integration site in the AKXD tumors, we screened the entire panel of AKXD tumors for virally induced rearrangements by using a genomic *Gfi-1* probe. Of the 283 tumors analyzed, 14 had virally induced rearrangements (Fig. 5; Table 2). Twelve of these tumors were T-cell lymphomas, while two were B-cell lymphomas. Only one of these tumors had a viral integration at *Evi-5*. These results are consistent with the previous studies of Gilks

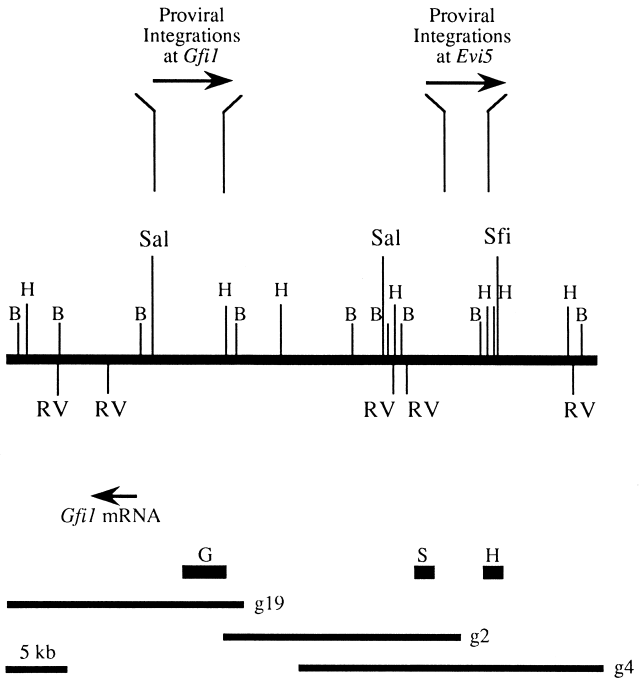

FIG. 4. Restriction map of the *Evi-5*–*Gfi-1* genomic region. Abbreviations for restriction endonucleases: B, *Bam*HI; H, *Hin*dIII; RV, *Eco*RV; Sal, *Sal*I; Sfi, *Sfi*I. Above the map, the positions and orientations (5′ to 3′) of proviral integrations at *Evi-5* and *Gfi-1* are indicated. Below the map, DNA probes used in Southern blot analysis are shown by the dark boxes; lambda clones spanning the region (g2, g4, and g19) are also shown. The start site and direction of *Gfi-1* transcription are indicated by an arrow.

and coworkers (16) suggesting that *Gfi-1* encodes a T-cell-specific proto-oncogene.

The positions and orientations of proviruses located at *Gfi-1* were determined as described above for the proviruses located at *Evi-5*. All of the proviruses were integrated within a 9-kb region of genomic DNA and, where determined, were oriented in the same transcriptional direction (Fig. 4). This transcriptional direction was identical to that of the proviruses located at *Evi-5* (Fig. 4). Proviral integration at *Gfi-1* was immediately upstream of the start site of *Gfi-1* transcription, and the direction of *Gfi-1* transcription was opposite to that of proviral transcription (Fig. 4). These results suggest that viral integration at *Gfi-1* upregulates *Gfi-1* transcription via an enhancer mechanism.

Second-site mutations in tumors with *Evi-5* or *Gfi-1* integrations. Ten of the AKXD tumors with viral integrations at

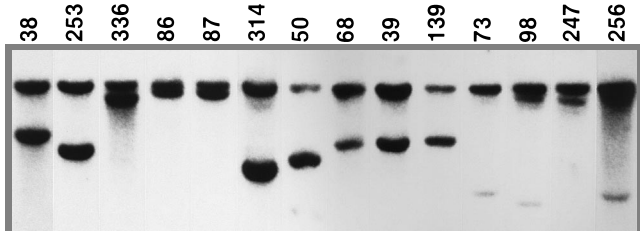

FIG. 5. *Gfi-1* rearrangements in AKXD tumors. *Eco*RV-digested tumor DNAs were analyzed by Southern blot hybridization with probe G. The designation of a tumor haboring a proviral integration at *Gfi-1* is listed above each lane. The unrearranged germ line *Eco*RV fragment is 22 kb, and the additional *Eco*RV fragments seen in each tumor indicate virus-induced rearrangements at *Gfi-1*.

TABLE 2. Virally induced rearrangements at the *Gfi-1* locus in AKXD tumors

Recombinant inbred strain	Tumor no.	Tumor type[a]	Second viral insertion
AKXD6	38	T	
AKXD10	253	T	
AKXD10	336	B	
AKXD14	86	B	
AKXD14	87	T	*Pim-1*
AKXD16	314	T	*Fis-1*
AKXD17	50	T	*Myc*
AKXD17	68	T	*Myc*
AKXD17	39	T	*Evi-5*
AKXD17	139	T	
AKXD18	73	T	*Myc*
AKXD18	98	T	*Myc*
AKXD21	247	T	
AKXD26	256	T	

[a] T, T-cell lymphoma; B, B-cell lymphoma.

Evi-5 or *Gfi-1* have previously been shown to contain viral integrations at other common integration sites, including *Myc*, *Mlvi-1*, *Pvt-1*, *Pim-1*, *Fis-1*, and *Evi-1* (Tables 1 and 2) (34, 36). All of these common sites, with the exception of *Evi-1*, have been causally implicated in murine T-cell lymphomagenesis (reviewed in references 6, 23, 38, and 47). These results are consistent with the notion that T-cell lymphomagenesis is a multistep disease which requires the cooperation of multiple different cellular proto-oncogenes and/or tumor suppressor genes. They are also consistent with the involvement of *Evi-5* and *Gfi-1* in T-cell disease.

The one exceptional tumor was AKXD-23 tumor 157 (Table 1), which has a viral integration at *Evi-5* in addition to the myeloid-tumor-cell-specific common integration site, *Evi-1* (36). Tumor 157 is a mixed myeloid and T-cell lymphoma; therefore, the simplest explanation for these results is that tumor 157 is oligoclonal, with one population of myeloid tumor cells harboring an *Evi-1* integration and a second population of T-cell tumor cells harboring an *Evi-5* integration.

DISCUSSION

In an attempt to identify novel myeloid-disease genes in BXH2 myelomonocytic tumors, we cloned a somatic provirus from a BXH2 tumor and investigated whether it was located at a common viral integration site. Unexpectedly, this provirus was not located at a common integration site in BXH2 tumors but was located at a common integration site in AKXD tumors. This common site, designated *Evi-5*, was rearranged predominantly in AKXD T-cell lymphomas; most AKXD B-cell and myeloid lymphomas did not harbor viral integrations at *Evi-5*. These results suggest that *Evi-5* harbors a disease gene that predisposes mice primarily to the development of T-cell disease.

At present, it is not clear why a provirus cloned from a BXH2 myelomonocytic tumor would identify a common integration site in AKXD T-cell lymphomas but not in BXH2 myeloid tumors. One possibility is that *Evi-5* harbors a disease gene that can participate in a variety of different hematopoietic diseases but that the preferred disease that results from viral integration at *Evi-5* is T-cell disease. This possibility is consistent with our identification of one AKXD B-cell lymphoma that harbors an *Evi-5* rearrangement. Another possibility is that this BXH2 tumor was misclassified and is actually a T-cell lymphoma rather than a myeloid tumor. While Southern analysis has failed to identify any T-cell receptor rearrangements in this tumor that might be indicative of a T-cell origin, similar analyses with a large panel of BXH2 tumors suggest that a few percent of the tumors are, in fact, T-cell tumors (data not shown). Thus, it is still conceivable that this tumor is T cell in origin.

Genetic and physical mapping studies showed that *Evi-5* is located approximately 18 kb upstream of *Gfi-1* on mouse chromosome 5. *Gfi-1* is a common viral integration site that was identified in Moloney MuLV-induced rat T-cell lymphomas. *Gfi-1* encodes a zinc finger protein which, when overexpressed, contributes to the emergence of IL-2-independent cells (16). Like *Evi-5*, *Gfi-1* is also a common viral integration site in AKXD T-cell lymphomas.

Ten of the AKXD T-cell lymphomas with viral integrations at *Evi-5* or *Gfi-1* also contained viral integrations at other common integration sites identified in mouse and rat T-cell lymphomas. While we have not yet proven that viral integration into these common sites occurs in the same tumor cell, as opposed to different subpopulations of tumor cells, these results are consistent with data from other laboratories indicating that T-cell lymphomagenesis is a multistep disease requiring the cooperation of many different disease genes (6).

Nine of the lymphomas with integrations in *Evi-5* or *Gfi-1* had integrations in *Myc* or in common sites that are located near and activate *Myc* (*Pvt-1*) (32, 43) or that synergize with *Myc* (*Pim-1*) (11, 42, 48). These results strongly suggest that *Gfi-1* and *Evi-5* can cooperate with *Myc* in tumor induction and are consistent with previous reports demonstrating that *Myc* is a frequent target of retroviral integration in mouse and rat T-cell lymphomas (38).

One of the lymphomas with an integration in *Gfi-1* also had an integration in *Fis-1. Fis-1* is a common site of Friend murine leukemia virus integration in mouse lymphomas and myelogenous leukemias (44). *Fis-1* has been localized at 50 to 300 kb 5′ of the cyclin D1 gene (*Ccnd-1*), and viral integration at *Fis-1* has been shown to upregulate expression of *Ccnd-1* in both myelogenous leukemias and T-cell lymphomas (29).

An important question that remains to be answered is whether viral integration at *Evi-5* merely serves to activate *Gfi-1* expression or whether *Evi-5* encodes a separate and distinct gene. At this point, the two alternative explanations seem equally feasible. As discussed above, viral integration at *Mlvi-1* and *Mlvi-4*, which map approximately 30 and 270 kb 3′ of *Myc*, respectively, has been shown to activate *Myc* expression (32). Likewise, integration at *Fis-1* can activate *Ccnd-1* expression even though *Ccnd-1* maps 50 to 300 kb 3′ of *Fis-1* (29). Viral integration therefore appears to be capable of affecting gene expression over very large distances. In contrast, viral integration at *Mis-2* and *Ahi-1*, which are located 160 and 35 kb, respectively, from *Myb* (26, 49), a frequent common integration site in murine myeloid leukemias (reviewed in reference 38), does not appear to alter *Myb* expression, suggesting that these two common sites harbor novel disease genes. Experiments are in progress to identify cell lines with viral integrations at *Evi-5* in order to determine whether *Evi-5* encodes a novel gene or affects *Gfi-1* expression at a distance.

Finally, the human homolog of *Gfi-1*, *GFI1*, has recently been mapped to human chromosome 1p22, defining a new syntenic region between mice and humans (4). This region has been implicated in a number of forms of human disease, including breast cancer, pheochromocytoma, malignant mesothelioma, and pleomorphic adenomas of the salivary gland. Future studies will be important to determine the role, if any, of *GFI1* and *EVI5* in human disease.

ACKNOWLEDGMENTS

This work was supported by the National Cancer Institute, DHHS, under contract with ABL.

We thank Carolyn Hustad and David Largaespada for helpful comments on the manuscript and Leighton Grimes and Philip Tsichlis for providing the *Gfi-1* probe.

REFERENCES

1. **Bedigian, H. G., D. A. Johnson, N. A. Jenkins, N. G. Copeland, and R. Evans.** 1984. Spontaneous and induced leukemias of myeloid origin in recombinant inbred BXH mice. J. Virol. **51:**586–594.
2. **Bedigian, H. G., L. A. Shepel, and P. C. Hoppe.** 1993. Transplacental transmission of a leukemogenic murine leukemia virus. J. Virol. **67:**6105–6109.
3. **Bedigian, H. G., B. A. Taylor, and H. Meier.** 1981. Expression of murine leukemia viruses in the highly lymphomatous BXH2 recombinant inbred mouse strain. J. Virol. **39:**632–640.
4. **Bell, D. W., T. Taguchi, N. A. Jenkins, D. J. Gilbert, N. G. Copeland, C. B. Gilks, P. Zweidler-McKay, H. L. Grimes, P. N. Tsichlis, and J. R. Testa.** 1995. Chromosomal localization of a gene, *GFI1*, encoding a novel zinc finger protein reveals a new syntenic region between man and rodents. Cytogenet. Cell Genet. **70:**263–267.
5. **Benovic, J. L., J. J. Onorato, J. L. Arriza, W. C. Stone, M. Lohse, N. A. Jenkins, D. J. Gilbert, N. G. Copeland, M. G. Caron, and R. J. Lefkowitz.** 1991. Cloning, expression and chromosomal localization of b-adrenergic receptor kinase 2: a new member of the receptor kinase family. J. Biol. Chem. **266:**14939–14946.
6. **Berns, A.** 1991. Tumorigenesis in transgenic mice: identification and characterization of synergizing oncogenes. J. Cell. Biochem. **47:**130–135.
7. **Buchberg, A. M., H. G. Bedigian, N. A. Jenkins, and N. G. Copeland.** 1990. *Evi-2*, a common integration site involved in murine myeloid leukemogenesis. Mol. Cell. Biol. **10:**4658–4666.
8. **Chattopadhyay, S. K., M. R. Lander, E. Rands, and D. R. Lowy.** 1980. Structure of endogenous murine leukemia virus DNA in mouse genomes. Proc. Natl. Acad. Sci. USA **77:**5774–5778.
9. **Chu, G., D. Vollrath, and R. W. Davis.** 1986. Separation of large DNA molecules by contour-clamped homogeneous electric fields. Science **234:** 1582–1585.
10. **Copeland, N. G., and N. A. Jenkins.** 1991. Development and applications of a molecular genetic linkage map of the mouse genome. Trends Genet. **7:**113–118.

10a. **Copeland, N. G., and N. A. Jenkins.** Unpublished results.

11. **Cuypers, H. T., G. Selten, W. Quint, M. Zijilstra, E. Robanus Maandag, W. Boelens, P. van Wezenbeek, C. Melief, and A. Berns.** 1984. Murine leukemia virus-induced T-cell lymphomagenesis: integration of proviruses in a distinct chromosomal region. Cell **37:**141–150.
12. **Evans, L. H.** 1986. Characterization of polytropic MuLVs from three-week-old AKR/J mice. Virology **153:**122–136.
13. **Evans, L. H., and F. G. Malik.** 1987. Class II polytropic murine leukemia viruses (MuLVs) of AKR/J mice: possible role in the generation of class I oncogenic polytropic MuLVs. J. Virol. **61:**1882–1892.
14. **Frankel, W. N., J. P. Stoye, B. A. Taylor, and J. M. Coffin.** 1989. Genetic identification of endogenous polytropic proviruses by using recombinant inbred mice. J. Virol. **63:**3810–3821.
15. **Gilbert, D. J., P. E. Neumann, B. A. Taylor, N. A. Jenkins, and N. G. Copeland.** 1993. Susceptibility of AKXD recombinant inbred mouse strains to lymphomas. J. Virol. **67:**2083–2090.
16. **Gilks, C. B., S. E. Bear, H. L. Grimes, and P. N. Tsichlis.** 1993. Progression of interleukin-2 (IL-2)-dependent rat T-cell lymphoma lines to IL-2-independent growth following activation of a gene (*Gfi-1*) encoding a novel zinc finger protein. Mol. Cell. Biol. **13:**1759–1768.
17. **Green, E. L.** 1981. Genetics and probability in animal breeding experiments, p. 77–113. Oxford University, New York.
18. **Hartley, J. W., N. K. Wolford, L. J. Old, and W. P. Rowe.** 1977. A new class of murine leukemia virus associated with development of spontaneous lymphomas. Proc. Natl. Acad. Sci. USA **74:**789–792.
19. **Herr, W., and W. Gilbert.** 1983. Somatically acquired recombinant murine leukemia proviruses in thymic leukemias of AKR/J mice. J. Virol. **46:**70–82.
20. **Herr, W., and W. Gilbert.** 1984. Free and integrated recombinant murine leukemia virus DNAs appear in preleukemic thymuses of AKR/J mice. J. Virol. **50:**155–162.
21. **Holland, C. A., J. W. Hartley, W. P. Rowe, and N. Hopkins.** 1985. At least four viral genes contribute to the leukemogenicity of murine retrovirus MCF247 in AKR mice. J. Virol. **53:**158–165.
22. **Hulsebos, T. J. M., N. A. Jenkins, D. J. Gilbert, and N. G. Copeland.** 1995. The b crystallin genes on human chromosome 22 define a new region of linkage homology with mouse chromosome 5. Genomics **25:**574–576.
23. **Ihle, J. N., K. Morishita, T. Matsugi, and C. Bartholomew.** 1990. Insertional mutagenesis and transformation of hematopoietic stem cells. Prog. Clin. Biol. Res. **352:**329–337.
24. **Jenkins, N. A., N. G. Copeland, B. A. Taylor, H. G. Bedigian, and B. K. Lee.** 1982. Ecotropic murine leukemia virus DNA content of normal and lymphomatous tissues of BXH2 recombinant inbred mice. J. Virol. **42:**379–388.
25. **Jenkins, N. A., N. G. Copeland, B. A. Taylor, and B. K. Lee.** 1982. Organization, distribution, and stability of endogenous ecotropic murine leukemia virus DNA sequences in chromosomes of *Mus musculus*. J. Virol. **43:**26–36.
26. **Jiang, X., L. Villeneuve, C. Turmel, C. A. Kozak, and P. Jolicoeur.** 1994. The *Myb* and *Ahi-1* genes are physically very closely linked on mouse chromosome 10. Mamm. Genome **5:**142–148.
27. **Justice, M. J., H. C. Morse III, N. A. Jenkins, and N. G. Copeland.** 1994. Identification of *Evi-3*, a novel common site of retroviral integration in mouse AKXD B-cell lymphomas. J. Virol. **68:**1293–1300.
28. **Kinsley, D. M., A. E. Bland, J. M. Grubber, P. C. Marker, L. B. Russell, N. G. Copeland, and N. A. Jenkins.** 1992. The mouse *short ear* skeletal morphogenesis locus is associated with defects in a bone morphogenetic member of the TGFβ superfamily. Cell **71:**399–410.
29. **Lammie, G. A., R. Smith, J. Silver, S. Brookes, C. Dickson, and G. Peters.** 1992. Proviral insertions near cyclin D1 in mouse lymphomas: a parallel for BCL1 translocations in human B-cell neoplasms. Oncogene **7:**2381–2387.
30. **Largaespada, D. A., J. D. Shaughnessy, Jr., N. A. Jenkins, and N. G. Copeland.** 1995. Retroviral integration at the *Evi-2* locus in BXH2 myeloid leukemia cell lines disrupts *NF1* expression without changes in steady state Ras-GTP levels. J. Virol. **69:**5095–5102.
31. **Larin, Z., A. P. Monaco, and H. Lehrach.** 1991. Yeast artificial chromosome libraries containing large inserts from mouse and human DNA. Proc. Natl. Acad. Sci. USA **88:**4123–4127.
32. **Lazo, P. A., J. S. Lee, and P. N. Tsichlis.** 1990. Long-distance activation of the *Myc* protooncogene by provirus insertion in *Mlvi1* or *Mlvi-4* in rat T-cell lymphomas. Proc. Natl. Acad. Sci. USA **87:**170–173.
33. **Lehrach, H., R. Drmanac, J. Hoheisel, Z. Larin, G. Lennon, A. P. Monaco, D. Nizetic, G. Zehetner, and A. Poustka.** 1990. Hybridization fingerprinting in genome mapping and sequencing, p. 39–81. *In* K. E. Davies and S. M. Tilghman (ed.), Genome analysis 1: genetic and physical mapping. Cold Spring Harbor Laboratory Press, Cold Spring Harbor, N.Y.
34. **Mucenski, M. L., D. J. Gilbert, B. A. Taylor, N. A. Jenkins, and N. G. Copeland.** 1987. Common sites of viral integration in lymphomas arising in AKXD recombinant inbred mouse strains. Oncogene Res. **2:**33–48.
35. **Mucenski, M. L., B. A. Taylor, N. G. Copeland, and N. A. Jenkins.** 1987. Characterization of somatically acquired ecotropic and mink cell focus-forming viruses in lymphomas of AKXD recombinant inbred mice. J. Virol. **61:**2929–2933.
36. **Mucenski, M. L., B. A. Taylor, J. N. Ihle, J. W. Hartley, H. C. Morse III, N. A. Jenkins, and N. G. Copeland.** 1988. Identification of a common ecotropic viral integration site, *Evi-1*, in the DNA of AKXD murine myeloid tumors. Mol. Cell. Biol. **8:**301–308.
37. **Mucenski, M. L., B. A. Taylor, N. A. Jenkins, and N. G. Copeland.** 1986. AKXD recombinant inbred strains: models for studying the molecular genetic basis of murine lymphomas. Mol. Cell. Biol. **6:**4236–4243.
38. **Peters, G.** 1990. Oncogenes at viral integration sites. Cell Growth Differ. **1:**503–510.
39. **Quint, W., W. Boelens, P. van Wezenbeek, T. Cuypers, E. R. Maandag, G. Selten, and A. Berns.** 1984. Generation of AKR mink cell focus-forming viruses: a conserved single-copy xenotrope-like provirus provides recombinant long terminal repeat sequences. J. Virol. **50:**432–438.
40. **Rose, M., F. Winston, and P. Hieter.** 1990. Methods in yeast Genetics. Cold Spring Harbor Laboratory Press, Cold Spring Harbor, N.Y.
41. **Sambrook, J., E. F. Fritsch, and T. Maniatis.** 1989. Molecular cloning: a laboratory manual, 2nd ed. Cold Spring Harbor Laboratory Press, Cold Spring Harbor, N.Y.
42. **Selten, G., H. T. Cuypers, W. Boelens, E. Robanus Maandag, J. Verbeek, J. Domen, C. van Beveren, and A. Berns.** 1986. The primary structure of the putative oncogene *pim-1* shows extensive homology with protein kinases. Cell **46:**603–611.
43. **Shtivelman, E., and J. M. Bishop.** 1990. Effects of translocations on transcription from *PVT*. Mol. Cell. Biol. **10:**1835–1839.
44. **Silver, J., and C. Kozak.** 1986. Common proviral integration region on mouse chromosome 7 in lymphomas and myelogenous leukemias induced by Friend murine leukemia virus. J. Virol. **57:**526–533.
45. **Stoye, J. P., and J. M. Coffin.** 1987. The four classes of endogenous murine leukemia virus: structural relationships and potential for recombination. J. Virol. **61:**2659–2669.
46. **Stoye, J. P., C. Moroni, and J. M. Coffin.** 1991. Virological events leading to spontaneous AKR lymphomas. J. Virol. **65:**1273–1285.
47. **van Lohuizen, M., and A. Berns.** 1990. Tumorigenesis by slow-transforming retroviruses—an update. Biochim. Biophys. Acta **1032:**213–235.
48. **van Lohuizen, M. S. Verbeek, P. Krimpenfort, J. Domen, C. Saris, T. Radaskiewicz, and A. Berns.** 1989. Predisposition to lymphomagenesis in *pim*-1 transgenic mice: cooperation with c-*myc* and N-*myc* in murine leukemia virus-induced tumors. Cell **56:**673–682.
49. **Villeneuve, L., X. Jiang, C. Turmel, C. A. Kozak, and P. Jolicoeur.** 1993. Long-range mapping of *Mis-2*, a common provirus integration site identified in murine leukemia virus-induced thymomas and located 160 kilobase pairs downstream of *Myb*. J. Virol. **67:**5733–5739.